J|A|C|S
ARTICLES
Published on Web 01/29/2002

The Short N−F Bond in N_2F^+ and How Pauli Repulsion Influences Bond Lengths. Theoretical Study of N_2X^+, NF_3X^+, and NH_3X^+ (X = F, H)

F. Matthias Bickelhaupt,*[,†,‡] Roger L. DeKock,*[,§,||] and Evert Jan Baerends[†]

Contribution from Afdeling Theoretische Chemie, Scheikundig Laboratorium der Vrije Universiteit, De Boelelaan 1083, NL-1081 HV Amsterdam, The Netherlands, and Department of Chemistry and Biochemistry, Calvin College, 3201 Burton Street SE, Grand Rapids, Michigan 49546-4388

Received July 23, 2001. Revised Manuscript Received November 8, 2001

Abstract: Exceptionally short N−F bond distances of only 1.217 Å (crystal) and 1.246 Å (gas phase) have been reported for N_2F^+, making it the shortest N−F bond ever observed. To trace the origin of this structural phenomenon, we have analyzed the model systems N_2X^+, NF_3X^+, and NH_3X^+ (X = F, H) using generalized gradient approximation density functional theory at BP86/TZ2P. In good agreement with experiment, the computations yield an extremely short N−F bond for N_2F^+: we find N−F bond distances in N_2F^+, NF_4^+, and NH_3F^+ of 1.245, 1.339, and 1.375 Å, respectively. The N−X bonding mechanisms are quantitatively analyzed in the framework of Kohn−Sham MO theory. At variance with the current hypothesis, reduced steric and other Pauli repulsion (of substituents or lone pairs at N with F) rather than the extent of s−p hybridization of N (i.e., sp versus sp^3) are responsible for the much shorter N−F distance in N_2F^+ compared to NF_4^+. The results for our nitrogen compounds are furthermore discussed in the more general context of how bond lengths are determined by both bonding and repulsive orbital interactions.

1. Introduction

Chemistry is replete with metonyms. We speak glibly about hybridization, electronic effects, steric interactions, etc. when we describe molecular structure and bonding. Some of these metonyms become so enshrined that we take them for granted. In the present paper, we wish to address the question of the relative N−F bond lengths in linear N_2F^+,[1−3] in tetrahedral NF_4^+,[4] and in tetrahedral NH_3F^+ (Chart 1, X = F). The latter molecule is strictly a theoretical construct, but the experimental N−F bond lengths in the first two are known from X-ray diffraction and mm-wave spectroscopy. Exceptionally short N−F bond distances of only 1.217 Å (crystal)[1] and 1.246 Å (gas phase)[2] have been reported for N_2F^+, making it, to our knowledge, the shortest N−F bond ever observed in an experiment. It is, for example, significantly shorter than the N−F bond of 1.30 Å in NF_4^+, which is already relatively short.[4] This has to be compared with N−F single-bond distances of 1.36, 1.41, and 1.52 Å in NF_3, N_2F_2, and NOF, respectively.[5]

Chart 1

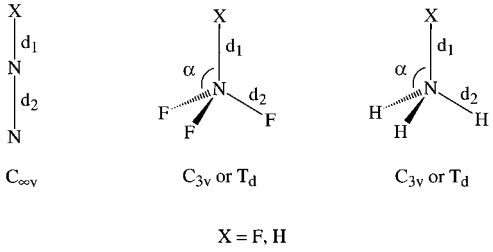

There is no doubt that the computational tools of the quantum chemist will be able to reproduce this bond length difference, and indeed we show that in this work. But our purpose in undertaking this study is not to show that we can reproduce experiment. Rather, we wish to know *why* these two bond lengths are so different and, in particular, *why* the N−F bond in N_2F^+ is so much shorter than that in NF_4^+.

Christe et al.[1] put forward the currently accepted rationale for the bond length difference quoted above, namely, that the shorter bond in N_2F^+ compared to NF_4^+ is due to the sp hybridization on the N atom in the former as compared to the sp^3 hybridization on N in the latter. This rationale suggests that the metonym "electronic" rather than "steric" is most important for the geometric feature of interest. Yet, the equilibrium bond length is the result of the interplay between both bonding and repulsive orbital interactions. Can the latter really be ignored?

* To whom correspondence should be addressed.
† Vrije Universiteit.
‡ Fax: +31−20−44 47629. E-mail: bickel@chem.vu.nl.
§ Calvin College.
|| Fax: +1-616-957 6501. E-mail: dekock@calvin.edu.

(1) Christe, K. O.; Wilson, R. D.; Wilson, W. W.; Bau, R.; Sukumar, S.; Dixon, D. A. *J. Am. Chem. Soc.* **1991**, *113*, 3795.
(2) Botschwina, P.; Sebald, P.; Bogley, M.; Demuynck, C.; Destombes, J.-L. *J. Mol. Spectrosc.* **1992**, *153*, 255.
(3) For a summary of literature on the N−F bond in N_2F^+, see: Cacace, F.; Grandinetti, F.; Pepi, F. *Inorg. Chem.* **1995**, *34*, 1325, and references therein.
(4) (a) Christe, K. O.; Lind, M. D.; Thorup, N.; Russell, D. R.; Bau, R. *Inorg. Chem.* **1988**, *27*, 2450. (b) Bettinger, H. F.; Schleyer, P. v. R.; Schaefer, H. F. *J. Am. Chem. Soc.* **1998**, *120*, 11439. (c) Christe, K. O.; Wilson, R. D.; Sawodny, W. J. *J. Mol. Struct.* **1971**, *8*, 245.
(5) (a) *Handbook of Chemistry and Physics*, 63rd ed.; Weast, R. C., Ed.; CRC Press: Boca Raton, FL, 1982−1983. (b) Greenwood, N. N.; Earnshaw, A. *Chemistry of the Elements*; Pergamon: Oxford, U.K., 1990; Chapter 11.

10.1021/ja0117837 CCC: $22.00

To trace the origin of the bond length differences, we have performed a generalized gradient approximation (GGA) density functional theory (DFT)[6] study on the model systems N_2X^+, NF_3X^+, and NH_3X^+ (X = F, H) shown in Chart 1. We analyze and interpret the bonding in the title molecules within the framework of the Kohn−Sham molecular orbital (MO) model.[7] This enables us to quantify intuitive concepts such as the electronic and hybridization effects, which can be associated with the bonding orbital interactions. But we also can quantify steric and other nonbonded interactions, which are caused by Pauli repulsive orbital interactions (vide infra). We also discuss possible implications of our results for carbon chemistry, i.e., for our conception about the role of hybridization and steric effects in determining the relative lengths of C−H and other C−X bonds.

2. Method

2.1. General Procedure. All calculations were carried out with the Amsterdam-density-functional (ADF) program developed by Baerends and others.[8] For a general overview of performance and possibilities of ADF, see ref 8a and literature cited therein. The MOs were expanded in a large uncontracted set of Slater-type orbitals (STOs) containing diffuse functions: TZ2P (no Gaussian basis functions are involved). The basis set is of triple-ζ quality, augmented with two sets of polarization functions: 3d and 4f on N and F and 2p and 3d on H. The 1s core shells of N and F were treated by the frozen-core approximation.[8a,b,d] An auxiliary set of s, p, d, f, and g STOs was used to fit the molecular density and to represent the Coulomb and exchange-correlation potentials accurately in each self-consistent field (SCF) cycle. The numerical integration was performed using the scheme of te Velde and Baerends.[8e]

Geometries were optimized using analytical gradient techniques.[8f] Energies were calculated at the BP86 level of the GGA: exchange is described by Slater's Xα potential,[6b] and correlation is treated in the Vosko−Wilk−Nusair (VWN) parametrization[8g] with gradient corrections to the exchange (Becke-88)[8h,i] and correlation (Perdew-86)[8j] added self-consistently.[8k] No zero-point vibrational energy (ZPE) corrections were applied.

2.2. Bond Analysis. The N−X bonding mechanisms in N_2X^+, NF_3X^+, and NH_3X^+ (X = F, H) were analyzed and interpreted in the framework of the Kohn−Sham MO model using a Morokuma-type decomposition of the bond energy into orbital and electrostatic interactions.[7,9] This was done for technical reasons at the BP86-P level at which nonlocal corrections are added as a perturbation to the result obtained with the local density approximation (LDA). BP86-P bond energies differ consistently by a few kilocalories per mole from the more accurate BP86 values (vide supra). To facilitate a straightforward comparison, the BP86-P results of the bond energy analysis were scaled to match exactly our more accurate BP86 bond energies. The overall bond energy ΔE is first divided into two major components:

$$\Delta E = \Delta E_{\text{prep}} + \Delta E_{\text{int}} \quad (1)$$

The preparation energy ΔE_{prep} is the amount of energy required to deform the separated fragments from their equilibrium structure to the geometry that they acquire in the composite molecule. The actual interaction energy ΔE_{int} between the prepared fragments can be further split up into three physically meaningful terms:

$$\Delta E_{\text{int}} = \Delta E_{\text{elst}} + \Delta E_{\text{Pauli}} + \Delta E_{\text{oi}} \quad (2)$$

Here, ΔE_{elst} corresponds to the classical electrostatic interaction between the unperturbed charge distributions of the prepared fragments and is usually attractive. The Pauli repulsion ΔE_{Pauli} comprises the four-electron destabilizing interactions between occupied orbitals and is responsible for any steric repulsion. The orbital interaction ΔE_{oi} accounts for electron-pair bonding, charge transfer (e.g. HOMO−LUMO interactions), and polarization (empty/occupied orbital mixing on one fragment due to the presence of another fragment). It can be decomposed into the contributions from the different irreducible representations of the molecular point group (e.g. the σ and the π bond in the present systems) using the extended transition-state (ETS) method developed by Ziegler and Rauk.[9a,b]

$$\Delta E_{\text{oi}} = \Sigma_\Gamma \Delta E_\Gamma = \Delta E_\sigma + \Delta E_\pi \quad (3)$$

Atomic charges were computed using the recently developed Voronoi deformation density (VDD)[10] method and the Hirshfeld[11] scheme.

Table 1. Calculated Homolytic N−F and N−H Bond Dissociation Energies BDE (kcal/mol) and Geometry Parameters d_1, d_2 (Å), and α (deg) of N_2X^+, NF_3X^+, and NH_3X^+ (X = F, H; see Chart 1)[a]

syst	BDE	d_1	d_2	α
N_2-F^+	102.5	1.245	1.112	
NF_3-F^+	70.3	1.339	1.339	109.47
NH_3-F^+	79.2	1.375	1.042	107.82
N_2-H^+	166.5[b]	1.045	1.096	
NF_3-H^+	111.2	1.054	1.342	109.90
NH_3-H^+	135.6	1.031	1.031	109.47

[a] BP86/TZ2P level. No ZPE correction. [b] For N_2H^+, the heterolytic BDE of 123.7 kcal/mol is lower than the homolytic BDE.

3. Results and Discussion

3.1. Structures and Bond Strengths. Our computed BP86/TZ2P geometries and homolytic bond dissociation energies (BDE) of N_2X^+, NF_3X^+, and NH_3X^+ (X = F, H) are collected in Table 1. In agreement with X-ray experimental investigations, we find that the N−F bond in N_2F^+ (1.245 Å) is substantially shorter than the one in NF_4^+ (1.339 Å). Our N−F bond distances of 1.245 and 1.339 Å, respectively, are systematically a few hundredths of an angstrom longer than the corresponding X-ray values of 1.217 [1] and 1.30 Å.[4a] This can be ascribed to the fact that the former refer to the gas phase, whereas the latter are subject to effects of the molecular environment in the crystal. Note for example that our N−F bond distance of 1.245 Å agrees virtually perfectly with the gas-phase value of 1.246 ± 0.001 Å obtained by Botschwina et al.[2] using mm-wave spectroscopy. The agreement is even somewhat better than that achieved by

(6) (a) Parr, R. G.; Yang, W. *Density-Functional Theory of Atoms and Molecules*; Oxford University Press: New York, 1989. (b) Slater, J. C. *Quantum Theory of Molecules and Solids*, Vol. 4; McGraw-Hill: New York, 1974.
(7) (a) Bickelhaupt, F. M.; Baerends, E. J. In *Reviews in Computational Chemistry*; Lipkowitz, K. B., Boyd, D. B., Eds.; Wiley-VCH: New York, 2000; Vol. 15, pp 1−86. (b) Stowasser, R.; Hoffmann, R. *J. Am. Chem. Soc.* **1999**, *121*, 3414. (c) Baerends, E. J.; Gritsenko, O. V. *J. Phys. Chem.* **1997**, *101*, 5383.
(8) (a) te Velde, G.; Bickelhaupt, F. M.; Baerends, E. J.; van Gisbergen, S. J. A.; Fonseca Guerra, C.; Snijders, J. G.; Ziegler, T. *J. Comput. Chem.* **2001**, 22, 931. (b) Fonseca Guerra, C.; Snijders, J. G.; te Velde, G.; Baerends, E. J. *Theor. Chem. Acc.* **1998**, *99*, 391. (c) Fonseca Guerra, C.; Visser, O.; Snijders, J. G.; te Velde, G.; Baerends, E. J. In *Methods and Techniques for Computational Chemistry*; Clementi, E., Corongiu, G., Eds.; STEF: Cagliari, Italy, 1995; pp 305−395. (d) Baerends, E. J.; Ellis, D. E.; Ros, P. *Chem. Phys.* **1973**, 2, 41. (e) te Velde, G.; Baerends, E. J. *J. Comput. Phys.* **1992**, 99, 84. (f) Versluis, L.; Ziegler, T. *J. Chem. Phys.* **1988**, 88, 322. (g) Vosko, S. H.; Wilk, L.; Nusair, M. *Can. J. Phys.* **1980**, 58, 1200. (h) Becke, A. D. *J. Chem. Phys.* **1986**, 84, 4524. (i) Becke, A. D. *Phys. Rev. A* **1988**, 38, 3098. (j) Perdew, J. P. *Phys. Rev. B* **1986**, 33, 8822. Erratum: Perdew, J. P. *Phys. Rev. B* **1986**, 34, 7406. (k) Fan, L.; Ziegler, T. *J. Chem. Phys.* **1991**, 94, 6057.
(9) (a) Bickelhaupt, F. M.; Nibbering, N. M. M.; van Wezenbeek, E. M.; Baerends, E. J. *J. Phys. Chem.* **1992**, *96*, 4864. (b) Ziegler, T.; Rauk, A. *Theor. Chim. Acta* **1977**, 46, 1. (c) Morokuma, K. *J. Chem. Phys.* **1971**, *55*, 1236.
(10) (a) Bickelhaupt, F. M.; van Eikema Hommes, N. J. R.; Fonseca Guerra, C.; Baerends, E. J. *Organometallics* **1996**, *15*, 2923. (b) Fonseca Guerra, C.; Bickelhaupt, F. M.; Snijders, J. G.; Baerends, E. J. *Chem. Eur. J.* **1999**, *5*, 3581.
(11) Hirshfeld, F. L. *Theor. Chim. Acta* **1977**, *44*, 129.

Table 2. Analysis of the N−F and N−H Bonds in $A-X^+$ ($A = N_2^{+\bullet}$, $NF_3^{+\bullet}$, $NH_3^{+\bullet}$; $X = F^\bullet$, $H^\bullet$)[a]

	N_2–F^+	NF_3–F^+	NH_3–F^+	N_2–H^+	NF_3–H^+	NH_3–H^+
Bond Energy Decomposition (kcal/mol)						
ΔE_σ	−284.7	−233.3	−208.3	−248.3	−230.3	−213.2
ΔE_π	−73.2	−43.6	−20.2	−11.6	−7.0	−2.8
ΔE_{oi}	−357.9	−276.9	−228.5	−259.9	−237.3	−216.0
ΔE_{elst}	−99.1	−95.9	−66.6	−43.8	−69.4	−47.4
ΔE_{Pauli}	354.5	297.9	206.2	136.7	190.3	116.0
ΔE_{int}	−102.5	−74.9	−88.9	−167.0	−116.4	−147.4
ΔE_{prep}	0.0	4.6	9.7	0.5	5.2	11.8
$\Delta E = -BDE$	−102.5	−70.3	−79.2	−166.5	−111.2	−135.6
Fragment Orbital Overlaps ⟨A|X⟩						
$\langle\sigma_{SOMO}\|\sigma_{SOMO}\rangle$	0.27	0.23	0.28	0.44	0.36	0.50
$\langle\sigma_{HOMO}\|\sigma_{SOMO}\rangle$	0.28	0.22	0.24	0.42	0.38	0.47
$\langle\pi_{HOMO}\|\pi_{HOMO}\rangle$	0.12	0.07	0.13			
$\langle\pi_{LUMO}\|\pi_{HOMO}\rangle$	0.18	0.14	0.02			
Fragment Orbital Populations (e)						
A: σ_{SOMO}	1.09	0.91	0.73	1.57	1.46	1.21
σ_{HOMO}	1.61	1.81	1.96	1.77	1.75	2.01
π_{HOMO}	1.98	2.00	1.99	1.97	1.99	1.97
π_{LUMO}	0.13	0.08	0.01	0.01	0.00	0.00
X: σ_{SOMO}	1.20	1.21	1.22	0.55	0.73	0.72
π_{HOMO}	1.87	1.91	1.97			
Atom X Charge (e)						
VDD	0.31	0.15	0.07	0.44	0.33	0.28
Hirshfeld	0.28	0.14	0.07	0.35	0.27	0.25

[a] BP86-P/TZ2P scaled to match BP86/TZ2P bond energies (see section 2.2).

high-level ab initio computations at the CEPA-1 level which arrive at slightly longer N−F distances of 1.2612 (basis A) and 1.2521 Å (basis C).[2] Also for NF_4^+ and NF_3H^+, the agreement with previous computational studies is satisfactory. The N−F bond length in NF_4^+ has been computed to be 1.339 Å (BP86/TZ2P, this study), 1.328 Å (B3LYP/6-311+G*),[4b] 1.304 Å (MP2/cc-pVTZ),[4b] and 1.311 Å (CCSD/ DZP).[4b] The N−H bond length in NF_3H^+ has been computed to be 1.054 Å (BP86/TZ2P, this study) and 1.041 Å (MP2(FU)/6-31G**).[12a]

The results for N_2F^+, NF_4^+, and NH_3F^+ seem to confirm, at first sight, the current explanation for the short N−F bond in N_2F^+, i.e., the more compact sp hybridized nitrogen atom of N_2F^+ compared to the more extended sp^3 hybridized nitrogen atom in NF_4^+. The N−F bond is short and strong in N_2F^+ (1.245 Å, BDE = 102.5 kcal/mol) and substantially longer (by 0.094 and 0.036 Å, respectively) and weaker in NF_4^+ (1.339 Å, BDE = 70.3 kcal/mol) and in NH_3F^+ (1.375 Å, 79.2 kcal/mol) which both have an sp^3 nitrogen atom. However, a breakdown of the current picture occurs if we compare the above N−F bonds with the analogous N−H bonds in N_2H^+, NF_3H^+, and NH_4^+. If the degree of s−p hybridization of the nitrogen atom involved in the N−X bond would indeed be decisive for the equilibrium bond length, one should find again the shortest N−H bond for N_2H^+ (sp hybridized N atom) and longer N−H bonds for NF_3H^+ and NH_4^+ (sp^3 hybridized N atoms). But this is not what we find (see Table 1). Instead, going from N_2H^+ (1.045 Å) to NF_3H^+ (1.054 Å), the N−H bond distances increase only slightly by 0.009 Å, and, going from N_2H^+ (1.045 Å) to NH_4^+ (1.031 Å), it even *decreases* by 0.014 Å.

3.2. The Role of Pauli Repulsion in the N−X Bonding Mechanisms. In the following, we try to understand these trends through detailed analyses of the electronic structure and bonding mechanism in the six model systems. The results of our Kohn−Sham MO analyses are summarized in Table 2 and Figures 1−3. In all systems, there is a net flow of electrons from the substituent X = H, F to the cationic, nitrogen-containing fragment, resulting in a positive atomic charge on X according to both the VDD and the Hirshfeld method (see Table 2). The main bonding interaction (vide infra) is provided by the σ electron-pair bond[7a,9a] (see **1**) between the singly occupied molecular orbital (SOMO) of $N_2^{+\bullet}$ ($3\sigma_g$), $NF_3^{+\bullet}$ ($4a_1$), or $NH_3^{+\bullet}$ ($2a_1$) on one side (see Figure 1) and the SOMO of $F^\bullet$ ($2p_\sigma$) or

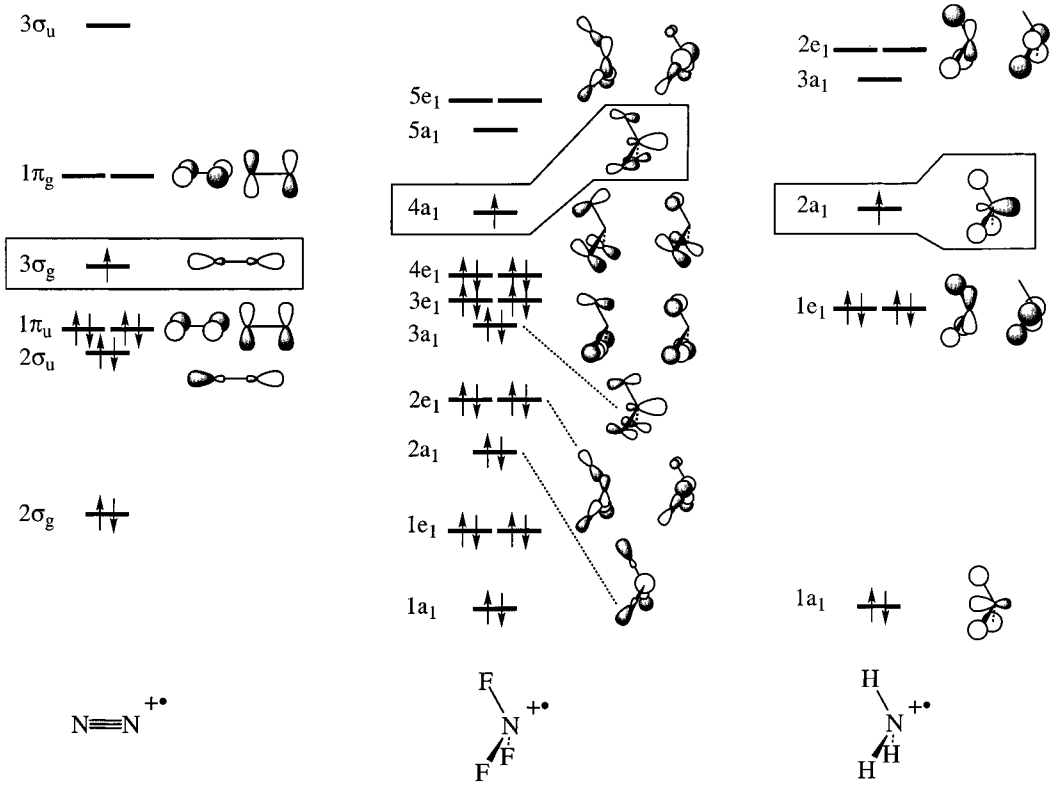

Figure 1. Valence MO scheme for N_2^+, NF_3^+, and NH_3^+.

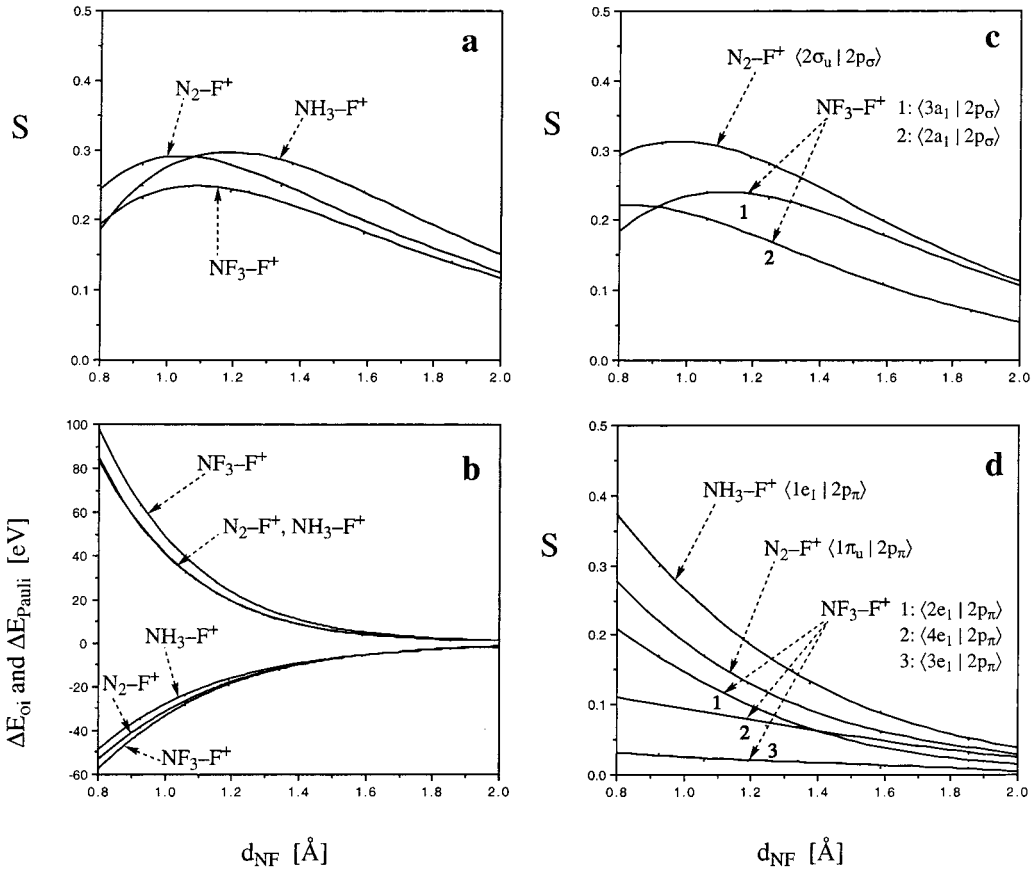

Figure 2. Selected bonding parameters as a function of the N−F bond distance in N_2−F^+, NF_3−F^+, and NH_3−F^+ (BP86-P/TZ2P level): (a) SOMO−SOMO overlaps, (b) Pauli repulsion (ΔE_{Pauli}) and orbital interaction (ΔE_{oi}), (c) closed-shell overlaps in σ symmetry, and (d) closed-shell overlaps in π symmetry. The equilibrium N−F bond distances are 1.245 (N_2−F^+), 1.339 (NF_3−F^+), and 1.375 Å (NH_3−F^+); see Table 1.

$H^\bullet$ (1s) on the other side. The N−F σ electron-pair bonds in N_2−F^+, NF_3−F^+, and NH_3−F^+ are all similar in polarity, actually not very polar at all, as reflected by the populations of the fluorine $2p_\sigma$ SOMO (1.20−1.21 e, see Table 2); this orbital gains about one-fifth of an electron if compared to the valence state of the isolated atom (1.00 e).[13] It is mainly the donor−acceptor interactions (see **2**)[7a] in π symmetry that are responsible for the positive charge on fluorine by transferring electrons back to the nitrogen fragment (vide infra).

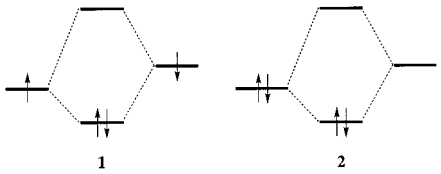

1 **2**

The overlaps corresponding with the σ electron-pair bonds are shown in Figures 2a and 3a as a function of the N−F and N−H bond distances, respectively. The overlap between the SOMO of $N_2^{+\bullet}$ ($3\sigma_g$, formally sp hybridized) and that of $F^\bullet$ (the $2p_\sigma$) reaches a maximum at shorter N−F bond distance than the overlap between the SOMO of $NF_3^{+\bullet}$ ($4a_1$, formally sp^3 hybridized) and that of $F^\bullet$ (see Figure 2a). This seems to point again toward the current model[1] for the short N−F bond in N_2F^+ which relates this structural phenomenon to the more compact nature of the sp lobe of the $N_2^{+\bullet}$ $3\sigma_g$ SOMO. Note however that all these maxima occur at N−F distances of ca. 1.0−1.2 Å (Figure 2a), well below the equilibrium bond lengths of ca. 1.2−1.4 Å (Table 1). The same holds for the N−H bonds: the maxima of the N−H electron-pair bond overlaps in N_2H^+, NF_3H^+, and NH_4^+ occur at bond distances below 0.8 Å (Figure 3a), whereas the equilibrium bond distances are 1.03−1.05 Å. This raises the question if the position of these bond overlap maxima is really decisive for the N−X equilibrium bond lengths. And, if not, which other mechanism is responsible?

To answer these questions, we take a closer look at the valence electronic structure of $N_2^{+\bullet}$ and $NF_3^{+\bullet}$. Figure 1 gives a schematic representation (i.e., in the right energetic order but not on scale) of the valence orbitals of these fragments as they emerge from our Kohn−Sham MO analyses. As can be seen, $N_2^{+\bullet}$ has a relatively small number of 9 valence electrons and, hence, only little closed-shell valence orbitals: $2\sigma_u$, $2\sigma_g$, and $1\pi_u$. On the other hand, $NF_3^{+\bullet}$ is with 25 valence electrons quite an electron-rich species and thus possesses more closed shells: $1a_1$, $2a_1$, $3a_1$, $1e_1$, $2e_1$, $3e_1$, and $4e_1$. One can therefore expect that the 2p and 2s atomic orbitals (AOs) of an incoming $F^\bullet$

(12) (a) Grandinetti, F.; Hrusák, J.; Schröder, D.; Karrass, S.; Schwarz, H. *J. Am. Chem. Soc.* **1992**, *114*, 2806. See also: (b) Fisher, J. J.; McMahon, T. B. *J. Am. Chem. Soc.* **1988**, *110*, 7599. (c) Reed, A. E.; Schleyer, P. v. R. *J. Am. Chem. Soc.* **1987**, *109*, 7362.

(13) (a) One of the reviewers has verified with ab initio calculations at MP2/6-311+G** that the N−F bonds in N_2−F^+, NF_3−F^+, and NH_3−F^+ are all similar in polarity and, actually, not very polar at all: (i) in a natural bond orbital (NBO) analysis, the N atom takes only 43.0, 43.4, and 41.7%, respectively, of the amplitude in the localized N−F bond orbital; (ii) in line with this, atoms in molecules (AIM) bond orders of 1.224, 1.387, and 1.140, respectively, confirm the strong N−F covalency. (b) For the NBO method see: Reed, A. E.; Curtiss, L. A.; Weinhold, F. *Chem. Rev.* **1988**, *88*, 899. (c) For the AIM method see: Bader, R. W. F. *Acc. Chem. Res.* **1985**, *18*, 9.

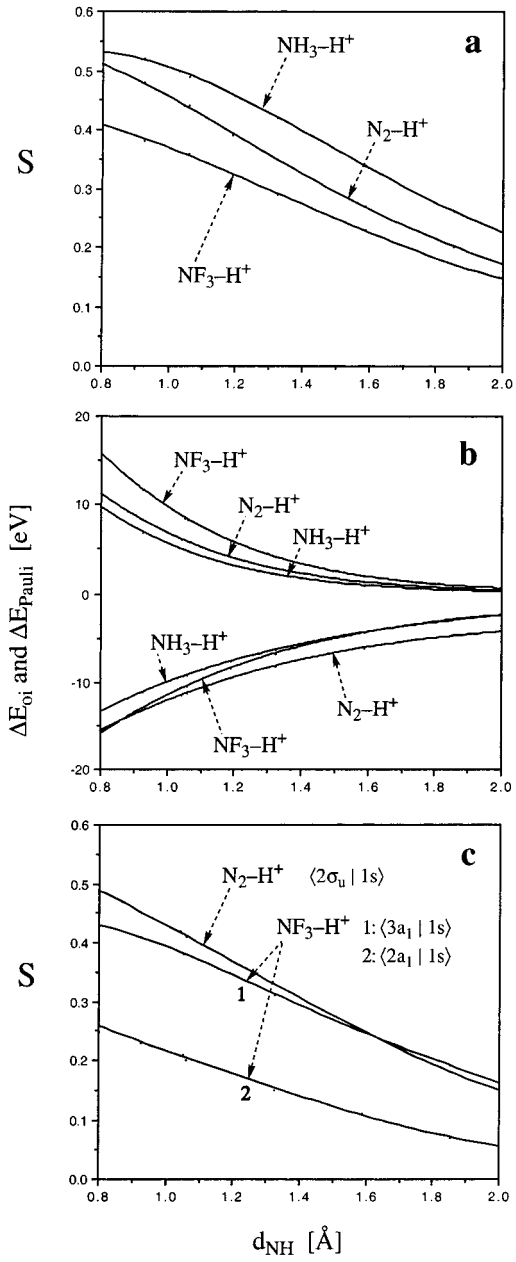

Figure 3. Selected bonding parameters as function of the N−H bond distance in N_2-H^+, NF_3-H^+, and NH_3-H^+ (BP86-P/TZ2P level): (a) SOMO−SOMO overlaps, (b) Pauli repulsion (ΔE_{Pauli}) and orbital interaction (ΔE_{oi}), and (c) closed-shell overlaps in σ symmetry. The equilibrium N−H bond distances are 1.045 (N_2-H^+), 1.054 (NF_3-H^+), and 1.031 Å (NH_3-H^+); see Table 1.

substituent experience a much stronger Pauli repulsion, i.e., 2-center, 3-electron (see **3**)[7a,14] and 2-center, 4-electron (see **4**)[7a,9a] repulsion with the larger number of closed shells of $NF_3^{+\bullet}$ than with $N_2^{+\bullet}$.

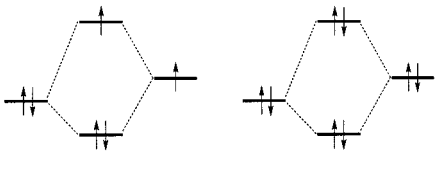

3 **4**

Indeed, this is confirmed by the quantitative bond energy decomposition (see section 2.2). But, at first sight, the results in Table 2 may suggest the opposite. Note, for example, that ΔE_{Pauli} is *less* repulsive for NF_3-F^+ (297.9 kcal/mol) than for N_2-F^+ (354.5 kcal/mol). One has to realize however that these values refer to equilibrium N−F bond lengths, which differ for the various species. This obscures the picture. For example, NF_3-F^+ has a longer equilibrium N−F bond distance than N_2-F^+, and it is not clear to what extent this is responsible for the smaller value of ΔE_{Pauli} (and all other components of the interaction ΔE_{int}) in the former (see Table 2). The situation becomes transparent only if we compare the Pauli repulsion ΔE_{Pauli} of the different species as a function of the N−F distance. This is done in Figure 2b, which displays the N−F Pauli repulsion ΔE_{Pauli} and bonding orbital interactions ΔE_{oi} of $N_2^{+\bullet}$ and $NF_3^{+\bullet}$ (and $NH_3^{+\bullet}$) with $F^\bullet$ as a function of the N−F distance. The corresponding overlaps of the most important Pauli repulsive orbital interactions with fluorine 2p orbitals are shown in Figure 2c,d.

The equilibrium bond distance is determined by the interplay of ΔV_{elst}, ΔE_{Pauli}, and ΔE_{oi} (see section 2.2). More precisely, it is determined by the relative slopes of the ΔV_{elst}, ΔE_{Pauli}, and ΔE_{oi} curves, that is, by how fast the values of these energy terms change as a function of the distance N−X between the molecular fragments. The magnitude as such of ΔV_{elst}, ΔE_{Pauli}, and ΔE_{oi} is not of importance. For example, the electrostatic component ΔV_{elst} of the various N−X bonds is not negligible with values of −47.4 up to −99.1 kcal/mol for NH_3-H^+ and N_2-F^+ (Table 2). Yet, because ΔV_{elst} appears to vary only weakly as a function of the N−X distance, it influences the equilibrium N−X bond distance only slightly. As explained below, the latter is therefore determined primarily by the balance between the slopes of the ΔE_{Pauli} and ΔE_{oi} curves shown in Figure 2b.

Figure 2b reveals the main trends (not the details) of the behavior of ΔE_{Pauli} and ΔE_{oi} as a function of the bond distance (ΔV_{elst} is not shown, for clarity). Note that the ΔE_{oi} curves of NF_3-F^+ and N_2-F^+ nearly coincide at equilibrium bond distance, the former being even slightly more bonding than the latter. This definitely rules out the current model that relates the N−F bond length to the degree of s−p hybridization. Instead, it is the ΔE_{Pauli} curve of NF_3-F^+, which is significantly more repulsive than the one of N_2-F^+, thus leading to a longer N−F bond in NF_4^+ than in N_2F^+. Note also that, as a consequence, the Pauli repulsion in the respective equilibrium distances is higher for N_2F^+ than for NF_4^+ (see Table 2).

This result once more highlights the importance of the Pauli repulsive orbital interactions in a modern MO model not only for accurately describing but also for correctly understanding structure (i.e., bond distances and angles) and the stability of molecular species (cf. refs 7a, 9a, and 15). But of course attractive orbital interactions are also an important factor in chemical bonding mechanisms. This is well illustrated by NH_3F^+, which has the longest N−F bond in the series N_2F^+, NF_3F^+, and NH_3F^+ (Table 1). This time, however, the bond is not long due to more repulsion. In fact, the $NH_3^{+\bullet}$ fragment yields essentially the same Pauli repulsion with $F^\bullet$ as $N_2^{+\bullet}$ (Figure 2b). This can be understood from the fact that $NH_3^{+\bullet}$

(14) Bickelhaupt, F. M.; Diefenbach, A.; de Visser, S. V.; de Koning, L. J.; Nibbering, N. M. M. *J. Phys. Chem. A* **1998**, *102*, 9549.
(15) (a) Bickelhaupt, F. M.; Ziegler, T.; Schleyer, P. v. R. *Organometallics* **1996**, *15*, 1477. See also: (b) See, R. F.; Dutoi, A. D.; McConnell, K. W.; Naylor, R. M. *J. Am. Chem. Soc.* **2001**, *123*, 2839.

(7 valence electrons) has, just as $N_2^{+\bullet}$ (9 valence electrons), a relatively small number of electrons and thus closed-shell valence orbitals: only $1a_1$ and $1e_1$ (see Figure 1). The long N−F bond in NH_3F^+ is caused by the weakness of the bonding orbital interactions ΔE_{oi} (Figure 2b), especially in π symmetry (see Table 2) between the occupied fluorine $2p_\pi$ AOs and the rather high-energy N−H antibonding $2e_1$ orbitals of $NH_3^{+\bullet}$ (see **2** and Figure 1). This is also reflected by the much smaller population that the π_{LUMO} of $NH_3^{+\bullet}$ (i.e., the $2e_1$, Figure 1) acquires in NH_3F^+ (0.02 e, Table 2) if compared to the π_{LUMO} of $N_2^{+\bullet}$ (i.e., the $1\pi_g$) in N_2F^+ (0.18 e) and the π_{LUMO} of $NF_3^{+\bullet}$ (i.e., the $5e_1$) in NF_4^+ (0.14 e).

It is instructive to carry out a numerical experiment in which all π orbital interactions, both bonding and repulsive, have been, in a sense, switched off. This can be achieved by comparing the series N_2X^+, NF_3X^+, and NH_3X^+ for X = F with that for X = H, because the hydrogen atom has, at variance with the fluorine atom, neither occupied nor unoccupied frontier orbitals in π symmetry. In the first place, not unexpectedly, all N−H bonds are typically shorter than the corresponding N−F bonds by 0.2−0.3 Å. This is primarily due to less Pauli repulsion with H because of the absence of lower lying closed-shell AOs on this atom (see Figure 1, and compare Figures 2b and 3b; note the different energy scales in the latter diagrams). Also, the electron-pair bond (see **1**) overlaps involving the hydrogen 1s AO are larger and continue to increase at shorter N−X distances than the corresponding overlaps involving the fluorine $2p_\sigma$ AO (compare Figures 2a and 3a). This is because the hydrogen 1s AO is more extended (causing overlap to build up already at longer N−X distances) and it has no nodal surface at the nucleus (which would otherwise cause cancellation of overlap at shorter N−X distances). The N−H bond in N_2H^+ (1.045 Å) turns out to be shorter than the one in NF_3H^+ (1.054 Å), analogous to the situation for X = F. This can be ascribed again to the fact that the NF_3−H^+ Pauli repulsion increases more strongly as the bond distance is reduced (see Figure 3b) because, as pointed out before, the $NF_3^{+\bullet}$ fragment simply has more σ closed-shell orbitals than $N_2^{+\bullet}$ (the important repulsive overlaps are shown in Figure 3c). Similar to the situation for NF_4^+ and N_2F^+, this Pauli repulsion effect overrules the trend in the bonding orbital interactions, which by itself favors a shorter N−H bond in NF_3H^+ than in N_2H^+ (see the steeper slope of ΔE_{oi} for NF_3H^+ around 1.1 Å in Figure 3b).

Interestingly, the N−H bond in NH_4^+ is the *shortest* N−X bond among those in N_2X^+, NF_3X^+, and NH_3X^+ for X = H (see Table 1) and not the longest one as we found for X = F. The reason is simply the absence in $NH_3^{+\bullet}$ of frontier closed-shell orbitals in σ symmetry (see Figure 1). Only at rather low energy, there is the $1a_1$ orbital, which is bonding between N, and all three H atoms of the $NH_3^{+\bullet}$ fragment. In addition, the H atom has no occupied orbitals in π symmetry that could enter into a Pauli repulsive 4-electron interaction with the $1e_1$ MOs of $NH_3^{+\bullet}$. All together, this leads to a very weak Pauli repulsion (Figure 3b) and, thus, to the short N−H bond in NH_4^+.

Finally, one can distinguish to a certain extent between two types of Pauli repulsive orbital interactions. The first one may be conceived as steric repulsion caused by the bulkiness of substituents at the nitrogen atom in the N−X bond. For example, the $3e_1$ and $4e_1$ orbitals of $NF_3^{+\bullet}$ have most of their amplitude on the three F atoms, not on the N atom (see Figure 1). The second type of Pauli repulsive orbital interactions originates from closed-shell orbitals with high amplitude on the nitrogen atom itself. These orbitals have the character of lone pairs (e.g., the $3a_1$ of $NF_3^{+\bullet}$ or the $2\sigma_u$ of $N_2^{+\bullet}$) or just (distorted) nitrogen AOs (e.g., the $2a_1$ or $2e_1$ of $NF_3^{+\bullet}$ or the $1e_1$ of $NH_3^{+\bullet}$). Of course, this distinction cannot always be made sharply, as there are many intermediate situations, i.e., fragment orbitals with sizable amplitude on both the central atom *and* the substituents.

4. Conclusions

The N−F bond in N_2F^+ is extremely short, even shorter than that in NF_4^+, because the $N_2^{+\bullet}$ fragment has fewer closed-shell orbitals in the vicinity of the N atom to which F binds than the $NF_3^{+\bullet}$ fragment. As a consequence, there are fewer N−F Pauli repulsive orbital interactions in N_2F^+ and the N−F equilibrium bond length can become much shorter. Our results, which are based on BP86/TZ2P computations, rule out the current conception that relates the relative N−F bond distances in N_2F^+ (sp) and NF_4^+ (sp^3) to the degree of s−p hybridization of the central N atom.

The results illustrate the importance of the Pauli repulsive orbital interactions ΔE_{Pauli} not only for accurately describing the system but also, in particular, for correctly understanding structure and bonding. Together with the bonding orbital interactions ΔE_{oi} (which in general receive much more attention in considerations of chemical bonds) and electrostatic interactions ΔV_{elst}, they determine the appearance (i.e., bond distances and angles) and stability of molecular species (see also refs 7a, 9a, and 15). We have emphasized that equilibrium bond lengths are determined by the relative slopes of ΔE_{Pauli}, ΔE_{oi}, and ΔV_{elst} as a function of the distance between the molecular fragments, and not by the magnitude of these energy terms. Furthermore, a distinction has been made between steric repulsion (i.e., Pauli repulsion with orbitals that have much amplitude on the substituents of the atoms involved in the bond, here the N atom) and repulsion with lone-pair (and other) orbitals that are more localized on the atoms themselves involved in the bond under consideration (here, the N and X = F, H atoms).

Our results also raise an important question. It is generally accepted in carbon chemistry that trends in C−X bond lengths are ruled by the percentage s-character of the carbon atom, e.g., sp vs sp^3 hybridization.[16] In view of our findings for N−X bonds, one may wonder if this picture is really valid and if steric effects are possibly much more important in determining relative lengths of C−H, C−F, and other C−X bonds than is currently believed.

Acknowledgment. We thank the National Computing Facilities (NCF) foundation of The Netherlands Organization for Scientific Research (NWO) for financial support. R.D.K. wishes to thank Calvin College for a Calvin Research Fellowship. We are also grateful to one of the reviewers for communicating to us the results cited in ref 13a.

JA0117837

(16) See, for example: (a) Carey, F. A.; Sundberg, R. J. *Advanced Organic Chemistry*, Part A; Plenum Press: New York, 1990; Chapter 1.2. (b) Streitwieser, A.; Heathcock, C. H.; Kosower, E. M. *Introduction to Organic Chemistry*; Macmillan: New York, 1992; Chapter 12.1.